Article

Ultrafast Nonadiabatic Dynamics of [Fe(bpy)] in Solution

Wojciech Gawelda, Andrea Cannizzo, Van-Thai Pham,
Frank van Mourik, Christian Bressler, and Majed Chergui

J. Am. Chem. Soc., **2007**, 129 (26), 8199-8206• DOI: 10.1021/ja070454x • Publication Date (Web): 09 June 2007

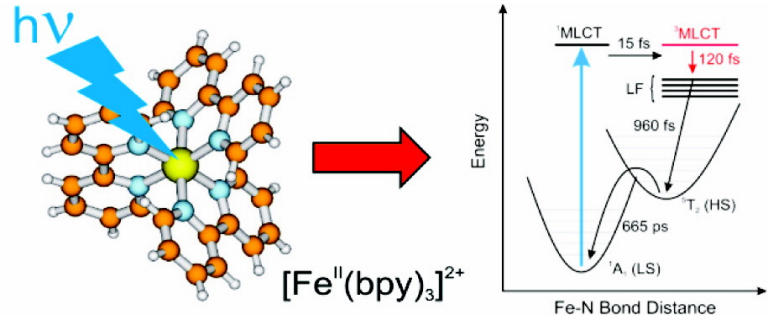

More About This Article

Additional resources and features associated with this article are available within the HTML version:

- Supporting Information
- Links to the 7 articles that cite this article, as of the time of this article download
- Access to high resolution figures
- Links to articles and content related to this article
- Copyright permission to reproduce figures and/or text from this article

View the Full Text HTML

J|A|C|S
ARTICLES
Published on Web 06/09/2007

Ultrafast Nonadiabatic Dynamics of $[Fe^{II}(bpy)_3]^{2+}$ in Solution

Wojciech Gawelda,[†,‡] Andrea Cannizzo,[†] Van-Thai Pham,[†] Frank van Mourik,[†] Christian Bressler,[†] and Majed Chergui*[,†]

Contribution from the Ecole Polytechnique Fédérale de Lausanne, Laboratoire de Spectroscopie Ultrarapide, Faculté des Sciences de Base, ISIC-BSP, CH-1015 Lausanne, Switzerland, and Paul Scherrer Institut, Swiss Light Source, CH-8092 Villigen, Switzerland

Received January 26, 2007; E-mail: majed.chergui@epfl.ch

Abstract: The ultrafast relaxation of aqueous iron(II)−tris(bipyridine) upon excitation into the singlet metal-to-ligand charge-transfer band (^{1}MLCT) has been characterized by femtosecond fluorescence up-conversion and transient absorption (TA) studies. The fluorescence experiment shows a very short-lived broad ^{1}MLCT emission band at ∼600 nm, which decays in ≤20 fs, and a weak emission at ∼660 nm, which we attribute to the ^{3}MLCT, populated by intersystem crossing (ISC) from the ^{1}MLCT state. The TA studies show a short-lived (<150 fs) excited-state absorption (ESA) below 400 nm, and a longer-lived one above 550 nm, along with the ground-state bleach (GSB). We identify the short-lived ESA as being due to the ^{3}MLCT state. The long-lived ESA decay and the GSB recovery occur on the time scale of the lowest excited high-spin quintet state $^5T_2$ lifetime. A singular value decomposition and a global analysis of the TA data, based on a sequential relaxation model, reveal three characteristic time scales: 120 fs, 960 fs, and 665 ps. The first is the decay of the ^{3}MLCT, the second is identified as the population time of the $^5T_2$ state, while the third is its decay time to the ground state. The anomalously high ISC rate is identical in $[Ru^{II}(bpy)_3]^{2+}$ and is therefore independent of the spin−orbit constant of the metal atom. To reconcile these rates with the regular quasi-harmonic vibrational progression of the ^{1}MLCT absorption, we propose a simple model of avoided crossings between singlet and triplet potential curves, induced by the strong spin−orbit interaction. The subsequent relaxation steps down to the $^5T_2$ state dissipate ∼2000 cm^{-1}/100 fs. This rate is discussed, and we conclude that it nevertheless can be described by the Fermi golden rule, despite its high value.

1. Introduction

Iron(II) molecular complexes have been extensively studied in relation to the spin crossover (SCO) phenomenon, where a transition from a low-spin (LS) ground state to a high-spin (HS) excited state is induced either by temperature or light, whereas the reverse transformation can, in addition, be induced by pressure. The study of SCO compounds is being actively pursued for their potential applications in magnetic data storage and as a basis for bistable devices.[1,2] In biology, SCO plays an important role in the dissociation and binding of ligands in heme proteins.[3,4]

In the family of iron(II) molecular complexes, iron(II)−tris(bipyridine), $[Fe^{II}(bpy)_3]^{2+}$, represents a LS complex, whose characteristic energy level scheme is shown in Figure 1. Contrary to most SCO complexes that have a relatively low adiabatic energy between LS and HS states, of the order of 100−1000 cm^{-1} such that SCO can be temperature induced, in $[Fe^{II}(bpy)_3]^{2+}$, it is ≈6000 cm^{-1} and the LS−HS transition can only be optically triggered, whereas the HS can be stabilized at cryogenic temperatures, in the so-called light-induced excited spin state trapping (LIESST) process.[5,6]

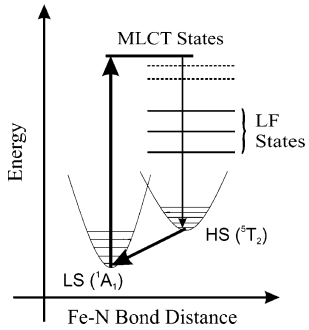

Figure 1. Simplified energy level scheme of $[Fe^{II}(bpy)_3]^{2+}$ showing the LS ground state, the lowest-lying HS excited state, and the intermediate MLCT and LF states.

In $[Fe^{II}(bpy)_3]^{2+}$, these states are the LS $^1A_1(t_{2g}^6)$ ground state and the HS $^5T_2(t_{2g}^4e_g^2)$ excited state, and the SCO transition changes the number of paired electrons in the t_{2g} sublevel of the HS state, with the unpaired electrons entering the e_g sublevel

[†] Ecole Polytechnique Fédérale de Lausanne.
[‡] Paul Scherrer Institut.

(1) Letard, J. F.; Guionneau, P.; Goux-Capes, L. *Spin Crossover Transition Met. Compd. III* **2004**, *235*, 221−249.
(2) Garcia, Y.; Moscovici, J.; Michalowicz, A.; Ksenofontov, V.; Levchenko, G.; Bravic, G.; Chasseau, D.; Gutlich, P. *Chem.−Eur. J.* **2002**, *8* (21), 4992−5000.
(3) Harvey, J. N. *Faraday Discuss.* **2004**, *127*, 165−177.
(4) Helbing, J.; Bonacina, L.; Pietri, R.; Bredenbeck, J.; Hamm, P.; van Mourik, F.; Chaussard, F.; Gonzalez-Gonzalez, A.; Chergui, M.; Ramos-Alvarez, C.; Ruiz, C.; Lopez-Garriga, J. *Biophys. J.* **2004**, *87* (3), 1881−1891.
(5) Hauser, A. *Spin Crossover Transition Met. Compd. II* **2004**, *234*, 155−198.
(6) Brady, C.; McGarvey, J. J.; McCusker, J. K.; Toftlund, H.; Hendrickson, D. N. *Spin Crossover Transition Met. Compd. III* **2004**, *235*, 1−22.

of the *d* orbitals and thus increasing the spin multiplicity to $S = 2$ (quintet state). Due to the transfer of two electrons to the antibonding e_g orbitals of the HS state and concurrent loss of π-backbonding from the t_{2g} orbitals, the Fe−N bond distance in the HS state is substantially elongated with respect to the LS value.

Similar to most other SCO compounds, the optical absorption spectrum of $[Fe^{II}(bpy)_3]^{2+}$ exhibits the characteristic and intense broad band centered at 523 nm, due to the singlet metal-to-ligand charge-transfer (^{1}MLCT) states (Figure 1). The kinetics of light-induced SCO has been characterized by conventional and ultrafast laser spectroscopy over the past few years.[5−10] Excitation of the ^{1}MLCT state leads to population of the lowest-lying (HS) quintet state, $^5T_2$, with almost unity quantum yield (Figure 1).[11,12] By monitoring spectral changes of iron(II)−polypyridine complexes, in regions where the difference spectra for the ligand-field and the charge-transfer states are of opposite signs (i.e., at 620 nm), Monat and McCusker[13] determined the depopulation of the charge-transfer manifold to occur within 80 ± 20 fs. Concerning the population time of the lowest $^5T_2$ state, they deduced that it occurs in <1ps, from a comparison of the femtosecond difference spectra at 0.5 and 6.3 ps with the anticipated difference spectrum for the LS to HS conversion.[13,14] Similar conclusions were recently drawn by Juban et al.[15] for the case of the $[Fe^{II}(bpy)_3]^{2+}$ complex.

The $^5T_2$ state is known to relax nonradiatively to the LS ground state in ∼0.65 ns in aqueous solutions at room temperature, as determined in ground-state bleaching recovery experiments.[14] Monat and McCusker[13] also found an 8 ps component in the bleach at 620 nm, which they attributed to vibrational relaxation within the $^5T_2$ state. However, the details of the intermediate steps going from the initially accessed ^{1}MLCT state to the $^5T_2$ state are still unknown. For example, whether the ^{3}MLCT manifold is involved in the initial relaxation pathway, like is the case in $[Ru^{II}(bpy)_3]^{2+}$,[16−18] has not been experimentally verified. In previous works, McCusker et al.[14] suggested that the population of the $^5T_2$ state is directly fed from the ^{1}MLCT state.

We recently investigated the initial events of the intramolecular dynamics from the ^{1}MLCT state in the somewhat similar $[Ru^{II}(bpy)_3]^{2+}$ complex using broad-band femtosecond fluorescence up-conversion spectroscopy.[16] We found that the intersystem crossing (ISC) occurs in ≤20 fs and populates the ^{3}MLCT, whose emission could also be detected. Given the similarity of the MLCT manifold in Ru and Fe complexes, this would suggest a similar mechanism for $[Fe^{II}(bpy)_3]^{2+}$. In addition, such an ISC rate, on the order of magnitude of high-frequency vibrational periods, is quite surprising. However, that such fast ISC processes can occur would explain the fast multiple ISC processes in the family of similar ferrous complexes, in particular, $[Fe^{II}(bpy)_3]^{2+}$.

In order to elucidate the details of the fast singlet to quintet relaxation in this complex, we combine our femtosecond polychromatic fluorescence up-conversion with femtosecond broad-band transient absorption (TA) spectroscopy. This approach, along with the decomposition of the TA data using singular value decomposition (SVD) and a global analysis (GA), allows us to fully map out the details of the relaxation cascade within the first picosecond and beyond. In particular, we show that the initial step of the relaxation is an ultrafast ISC, similar to that found in $[Ru^{II}(bpy)_3]^{2+}$,[16] leading to population of the ^{3}MLCT. Finally, we propose a simple model that reconciles the ultrafast ISC and the spectroscopic observations, which could be general to other metal-based complexes. The experimental setups and methods, as well as the details of the SVD and GA analysis, are described in detail in refs 16, 19, and 20 and in the Supporting Information.

2. Results

2.1. Femtosecond Polychromatic Fluorescence Up-Conversion. Figure 2a shows a typical two-dimensional (2D) fluorescence spectrum obtained upon excitation of aqueous $[Fe^{II}(bpy)_3]^{2+}$ at 400 nm. These have been corrected for group velocity dispersion (GVD, see the Supporting Information). Cuts at fixed times provide time-dependent emission spectra, which are shown in Figure 2b, while cuts at fixed emission wavelength provide the kinetic traces, shown in Figure 2c. Emission shows up in the 500−650 nm region already at $t = 0$. It is very short-lived, as it is instrument response limited (∼120 fs). Also, the width of the band does not change during the (short) lifetime of the emission. Note that in Figure 2a, a weak emission shows up at $\lambda \geq 650$ nm and $t \geq 100$ fs. This is confirmed in Figure 2b, where the spectrum at $t = 100$ fs exhibits two weak bands of almost identical intensity, one centered at ∼600 nm, the other at ∼660 nm. The former is a remnant of the main emission at earlier times, the latter is a new short-lived emission band, which we later identify as the ^{3}MLCT emission. We also verified that no other emissions occur at longer times, by recording scans up to 250 ps time delay. The comparison of Raman and emission time traces (Figure 2c) suggests a rise and a decay of the fluorescence almost within the cross-correlation of our experiment (∼110 fs) for all kinetic traces at <650 nm. However, at longer wavelengths, the rise of the signal is delayed, in agreement with parts a and b of Figure 2.

These results bear some analogy with those of $[Ru^{II}(bpy)_3]^{2+}$.[16] The 600 nm centered emission in Figure 2a is Stokes-shifted with respect to the ^{1}MLCT absorption by ∼2600 cm^{-1}, which is close to the corresponding value found for $[Ru^{II}(bpy)_3]^{2+}$ (∼3000 cm^{-1}). The kinetic traces at <650 nm in Figure 2b are best fitted with an exponential decay of 20 ± 5 fs convoluted with the instrumental response, which is similar

(7) Gutlich, P.; Garcia, Y.; Goodwin, H. A. *Chem. Soc. Rev.* **2000**, *29* (6), 419−427.
(8) Gutlich, P.; Goodwin, H. A. *Spin Crossover Transition Met. Compd. I* **2004**, *233*, 1−47.
(9) Hauser, A. *Coord. Chem. Rev.* **1991**, *111*, 275−290.
(10) Hauser, A.; Enachescu, C.; Daku, M. L.; Vargas, A.; Amstutz, N. *Coord. Chem. Rev.* **2006**, *250* (13−14), 1642−1652.
(11) Bergkamp, M. A.; Chang, C. K.; Netzel, T. L. *J. Phys. Chem.* **1983**, *87* (22), 4441−4446.
(12) Bergkamp, M. A.; Brunschwig, B. S.; Gutlich, P.; Netzel, T. L.; Sutin, N. *Chem. Phys. Lett.* **1981**, *81* (1), 147−150.
(13) Monat, J. E.; McCusker, J. K. *J. Am. Chem. Soc.* **2000**, *122* (17), 4092−4097.
(14) McCusker, J. K.; Walda, K. N.; Dunn, R. C.; Simon, J. D.; Magde, D.; Hendrickson, D. N. *J. Am. Chem. Soc.* **1993**, *115* (1), 298−307.
(15) Juban, E. A.; Smeigh, A. L.; Monat, J. E.; McCusker, J. K. *Coord. Chem. Rev.* **2006**, *250* (13−14), 1783−1791.
(16) Cannizzo, A.; van Mourik, F.; Gawelda, W.; Zgrablic, G.; Bressler, C.; Chergui, M. *Angew. Chem., Int. Ed.* **2006**, *45*, 3174−3176.
(17) Wallin, S.; Davidsson, J.; Modin, J.; Hammarstrom, L. *J. Phys. Chem. A* **2005**, *109* (21), 4697−4704.
(18) Tarnovsky, A.; Gawelda, W.; Johnson, M.; Bressler, C.; Chergui, M. *J. Phys. Chem. B* **2006**, *110* (51), 26497−26505.
(19) Zgrablic, G.; Voitchovsky, K.; Kindermann, M.; Haacke, S.; Chergui, M. *Biophys. J.* **2005**, *88* (4), 2779−2788.
(20) Gawelda, W. *Time-Resolved X-ray Absorption Spectroscopy of Transition Metal Complexes*; Ph.D. Thesis, EPFL: Lausanne, Switzerland, 2006.

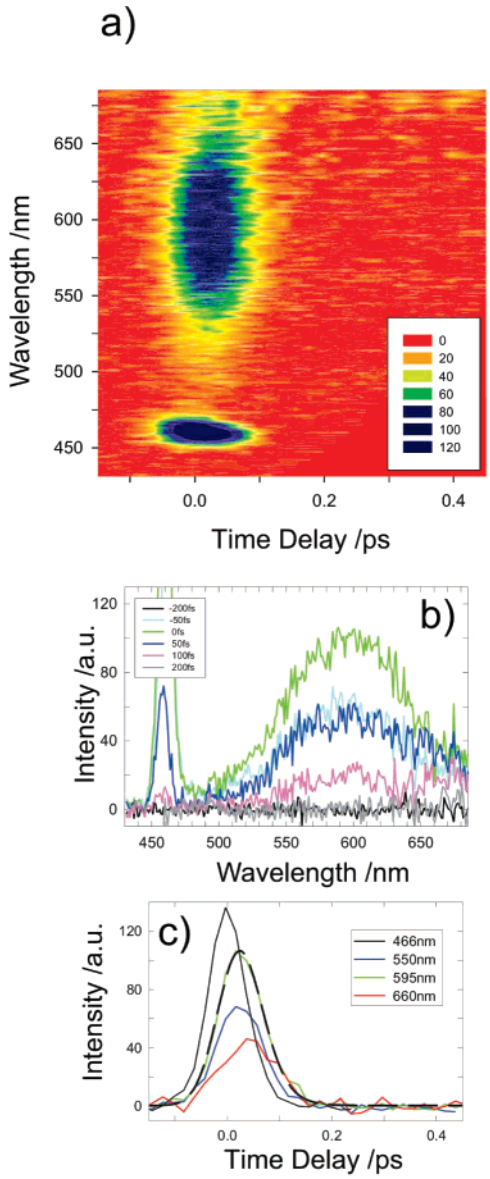

Figure 2. (a) Two-dimensional plot of time-resolved luminescence spectra of aqueous $[Fe^{II}(bpy)_3]^{2+}$ under excitation at 400 nm. The signal at 466 nm is the Raman line of water. (b) Luminescence spectra recorded at different time delays. (c) Time traces at different wavelengths. Time delays are taken with respect to the water Raman line (466 nm, not shown). The trace at 595 nm is shown together with its fit function (see text for more details).

to what we found in the case of $[Ru^{II}(bpy)_3]^{2+}$.[16] On the basis of these observations, we attribute the 600 nm emission to the short-lived ^{1}MLCT state. In $[Ru^{II}(bpy)_3]^{2+}$, the ^{1}MLCT emission decayed directly to the long-lived ^{3}MLCT state, which was clearly identified by its band centered at 620 nm. In the case of $[Fe^{II}(bpy)_3]^{2+}$, no triplet emission was ever reported in the literature, but we believe the short-lived weak emission centered at 660 nm is due to ^{3}MLCT emission, whose decay occurs within 100−150 fs.

In summary, the fluorescence up-conversion studies establish the ISC from ^{1}MLCT to ^{3}MLCT at a rate of $(20 \pm 5\ \text{fs})^{-1}$, just as in the Ru complex, and the subsequent decay of the ^{3}MLCT on a <150 fs time scale. The noise in Figure 2c, and the typical error of tens of femtoseconds on the GVD correction, could weaken the latter assignment, but it is confirmed by our TA measurements which also identify subsequent steps of the relaxation cascade down to the lowest quintet state.

2.2. Femtosecond Broad-Band Transient Absorption Spectroscopy. Figure 3 shows a representative set of 2D TA data of a 9 mM aqueous solution of $[Fe^{II}(bpy)_3]^{2+}$. Slices at either fixed time delay or fixed wavelength (see lines) deliver the corresponding spectra (at a given time delay, i.e., 5 ps) and kinetics (at a given wavelength, i.e., 523 nm), respectively, which are shown in the right panels. In the present study, we have investigated the TA spectra in three different time windows, namely, up to 5 ps, 20 ps, and 1 ns, respectively. The GVD correction (see the Supporting Information) was applied to all the data presented in the following sections.

Figure 4 shows representative TA spectra recorded at various time delays within the first 1.5 ps following photoexcitation. The evolution of the spectra shows a short-lived excited-state absorption (ESA, positive signal) in the 340−440 nm, whereas in the 560−640 nm range, it is longer lived. In <200 fs, the short-wavelength ESA is replaced by a negative signal, which we identify as the ground-state bleach (GSB) signal, by comparing the spectrum at 1.5 ps with the ground-state absorption spectrum. No signature of stimulated emission is observed around $t = 0$ and $\lambda_{em} \approx 600$ nm, which supports our estimate of the lifetime of the ^{1}MLCT of <20 fs. It is interesting to note that the short-lived ESA at <400 nm is similar to what we found in $[Ru^{II}(bpy)_3]^{2+}$,[18] which we attributed to the ^{3}MLCT absorption. This is further confirmed by the analysis below.

Additional information is contained in the kinetic traces, which for three characteristic wavelengths (370, 523, and 640 nm) are shown in Figure 5. Figure 5a shows the temporal evolution of the GSB signal in the 20 ps time window. It can be seen that this signal appears within the experimental temporal resolution of 140 fs and is followed by a weak partial recovery within the first 3−4 ps. At long delay times and as already known,[6,21] we find that the GSB disappears on a time scale of 665 ps.

Figure 5b shows the kinetics at 370 and 640 nm in the same time window as Figure 5a, while the inset zooms into the first 3.5 ps. These time traces are typical of the temporal response encountered in the spectral ranges where ESA signals were detected. The 370 nm trace reflects what we observe in Figure 4, i.e., a short-lived ESA, superimposed on the GSB. The 640 nm trace also shows a short-lived ESA component, which is comparable to that at 370 nm (see inset). We see that within the pump pulse duration (neat H_2O response measured under identical experimental conditions) no detectable time delay between the signals in the blue-most and red-most sides of the spectrum (with respect to the GSB signal) is observed. This short-lived component at the red side is immediately followed by a long-lived ESA.

The long-time transient spectra for time delays from 50 ps to 1 ns show that the spectral shape remains unchanged and follow the same time evolution as the GSB signal (Supporting Information Figure S2), with a recovery time of ∼665 ps. This suggests that the ESA signal on the red side is due to a quintet−quintet transition from the lowest $^5T_2$ state. In addition, in their low-temperature studies on $Fe(ptz)_6(BF_4)_2$ crystals using LIESST, Hauser[5] detected a broad quintet−quintet transition peaking

(21) McCusker, J. K.; Walda, K. N.; Dunn, R. C.; Simon, J. D.; Magde, D.; Hendrickson, D. N. *J. Am. Chem. Soc.* **1992**, *114* (17), 6919−6920.

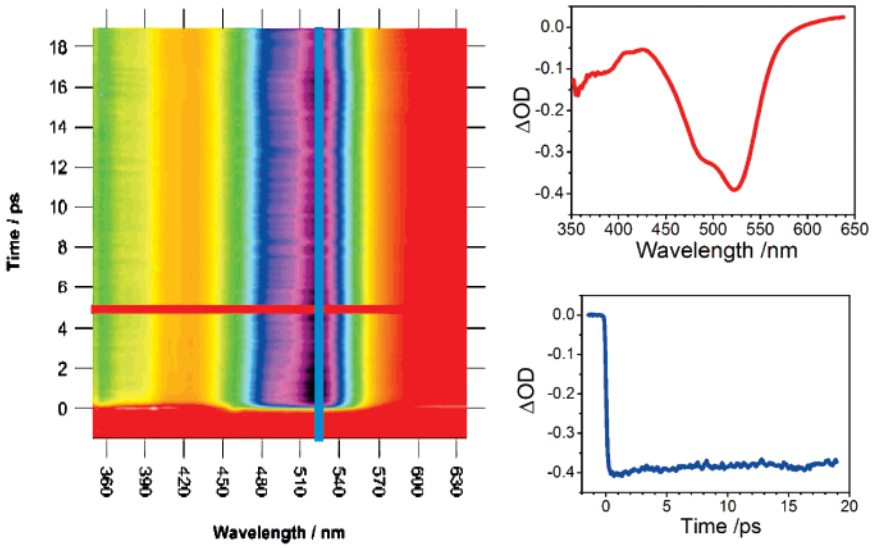

Figure 3. Two-dimensional TA data of a 9 mM aqueous solution of $[Fe^{II}(bpy)_3]^{2+}$ excited at 400 nm with a 140 fs pulse. The horizontal and vertical lines indicate the positions at which the temporal and spectral (at a given time delay, i.e., 5 ps) slices (right-hand side of the figure) were taken, respectively. The color codes in the left panel go from a strong bleach (purple) to no change (red); see also Figure 4.

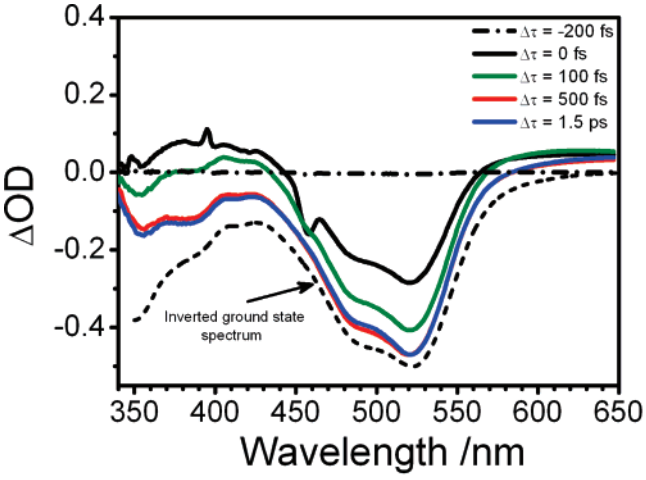

Figure 4. Representative transmission spectra of a 9 mM sample of aqueous $[Fe^{II}(bpy)_3]^{2+}$ within the first 1.5 ps after the photoexcitation at 400 nm. The peak around 400 nm at $t = 0$ is the residual scattered light contribution from the pump pulse. The strong negative absorption feature present in the early spectra around 450−460 nm is the impulsively induced Raman signal of H_2O. The dashed trace shows the inverted ground-state spectrum.

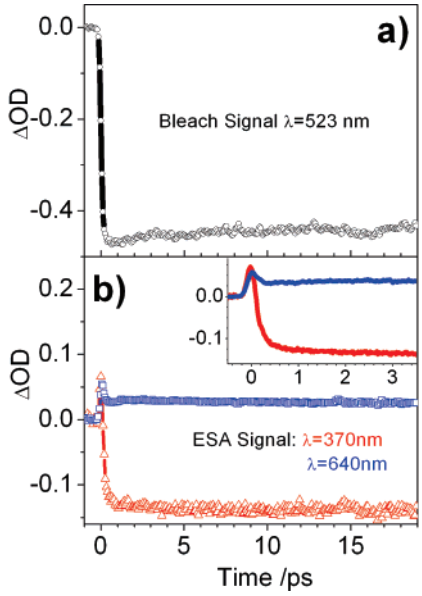

Figure 5. Representative kinetic traces recorded in a 20 ps window: (a) ground state bleach signal at 523 nm; (b) characteristic time traces in the blue-most (370 nm) and the red-most (640 nm) parts of the spectra in Figure 4. The inset zooms into the initial 3.5 ps time window and shows that both ESA signals occur simultaneously within the excitation pulse.

at ~830 nm. At 630 nm, we are probably probing the blue wing of a similar absorption in aqueous $[Fe^{II}(bpy)_3]^{2+}$.

It has previously been shown that ^{1}MLCT photoexcitation populates the long-lived HS state with nearly unity quantum yield.[11,12] Moreover, wavelength-selective excitation into the lower-lying weakly absorbing $^3T_2$ and $^3T_1$ LF states in low-temperature $Fe(ptz)_6(BF_4)_2$ crystals[22] shows no relaxation from these states to the ground state so that the entire population ends up in the lowest $^5T_2$ state. Therefore, Supporting Information Figure S2 directly links the observed GSB recovery signal to the decay of the HS excited state.

3. Spectral Decomposition

On the basis of the above results, it is fair to assume a sequential kinetic scheme for the relaxation from the ^{1}MLCT to the $^5T_2$ state, then to the ground state, in which the temporal evolution of the system can be described by a sequence of events with specific first-order decay rates k_i and corresponding lifetimes τ_i. In order to analyze the TA data shown in Figure 3, we have employed the GA approach discussed in detail in the Supporting Information.

This analysis has been applied to the results obtained in the three different time windows, namely, 5 ps, 20 ps, and 1 ns. The SVD-reconstructed data sets were fitted using a global fit approach, meaning that kinetic traces at all measured wavelengths could be fitted at once using identical model functions with the same lifetime decay constants. In the case of the results shown in Figure 5, the TA absorption kinetic traces were modeled with a sum of exponential functions convoluted with the instrument response function, as explained in the Supporting Information.

(22) Hauser, A. *J. Chem. Phys.* **1991**, *94* (4), 2741−2748.

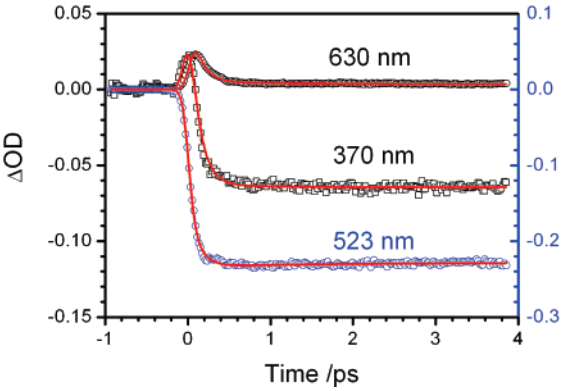

Figure 6. Kinetic traces of a 9 mM aqueous solution of $[Fe^{II}(bpy)_3]^{2+}$ complex upon 35 mJ/cm^2 excitation fluence in the 5 ps time window at three selected wavelengths, together with their fit functions using a global fit model (see text and Supporting Information for further details)

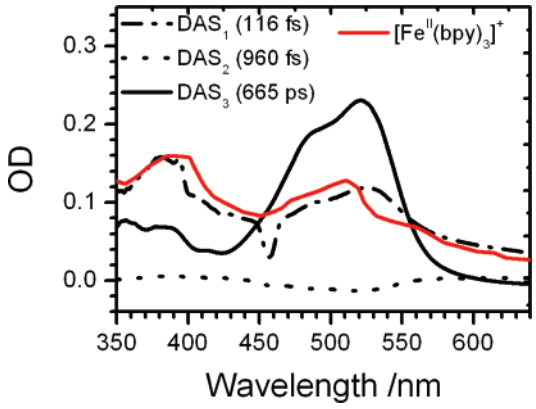

Figure 7. Decay-associated spectra extracted from the TA data, recorded at a pump fluence of 35 mJ/cm^2 (Figure 4), after the SVD transformation (see the Supporting Information). The spectrum of the reduced $[Fe^{II}(bpy)_3]^{+}$ complex (from ref 24) is plotted in red.

If we consider the long time window (up to 1 ns time delay), we find only one pronounced singular value, with a lifetime of 665 ± 35 ps, and its decay-associated spectrum (DAS) perfectly reproduces the ground-state absorption spectrum, as expected. This shows that at time delays >20 ps, the only relevant photoproduct is the $^5T_2$ state, associated to the GSB signal. This result provides important input for the subsequent analysis at shorter times.

In Figure 6 we show the kinetic traces at the three characteristic wavelengths with their fits. The fit functions obtained using the relaxation model described in the Supporting Information, delivered three time constants: 116 ± 10 fs, 960 ± 100 fs, and 665 ± 35 ps. Figure 7 shows the DAS corresponding to these three decay components. They were obtained using the preexponential coefficients $a_{i,k}$ of the global fit function and the spectral weights of each involved singular value (see the Supporting Information, eqs SI.4 and SI.5) in the detected spectral range. Therefore, the DAS reflect the relative spectral contributions for each time component in the measured TA data.

DAS_1 in Figure 7 is associated with the shortest time component ($\tau_1 \approx 120$ fs). It shows the characteristic ESA in the blue-most part of the spectrum and is compared to the static spectrum of the reduced complex taken from ref 23. There is a very good correspondence between the two spectra, and with the spectrum of the ESA from ^{3}MLCT in $[Ru^{II}(bpy)_3]^{2+}$.[18] This means that the initial excitation into the ^{1}MLCT manifold is followed by an ISC into the ^{3}MLCT manifold. DAS_2, associated to the 960 fs component, is very weak, at most between 5% and 10% of the total weight in SVD analysis, and its kinetics is superimposed on the GSB signal, which may suggest that the emerging HS absorption spectrum overlaps strongly with that of the LS ground-state complex. Hauser[22] have measured the absorption spectra of some of the intermediate LF states in a similar SCO complex in a low-temperature crystal and have estimated their corresponding cross sections to be 10^2−10^3 times weaker than the $^1A_1 \rightarrow {}^1$MLCT transition. Finally, for the last and longest component, the DAS_3 purely reflects the ground-state absorption, as expected. In summary, the SVD and GA of our data shows that the entire kinetics can be accounted for by three time constants, whose origin we discuss next, along with the femtosecond fluorescence results.

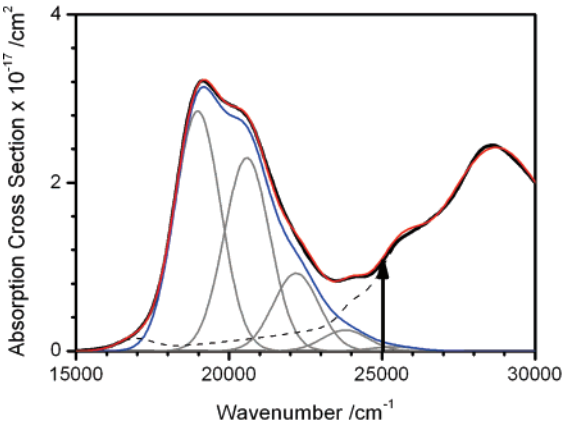

Figure 8. Steady-state absorption spectrum of an aqueous room-temperature $[Fe^{II}(bpy)_3]^{2+}$ complex (black line). The total fit (red line) and its various components, including the Franck−Condon progression of the 1607 cm^{-1} mode (blue line) and the residual background (dashed black line), are shown (see text for further details). The excitation energy is indicated by the vertical arrow at ca. 25 000 cm^{-1} (400 nm).

4. Discussion

4.1. Initial Franck−Condon Configuration and Charge-Transfer States. Figure 8 shows the absorption spectrum of aqueous room-temperature $[Fe^{II}(bpy)_3]^{2+}$ in the region of the ^{1}MLCT band. Similar to the case of $[Ru^{II}(bpy)_3]^{2+}$,[16] we fitted it with a progression of the high-frequency (1607 cm^{-1}) skeleton mode of bpy, assuming a Huang−Rhys factor of 0.8. The existence of such a progression is supported by low-temperature measurements in crystals.[5] We also added contributions from the ^{3}MLCT absorption and higher electronic excited states. Although this fit reliably reproduces the spectrum, it is by no means unique, and while a systematic analysis of the low-temperature spectra has not yet been done, we can suspect that there are more high-frequency progressions underneath the ^{1}MLCT absorption band, as in the case of the analogue Ru complex,[24] with the 1607 cm^{-1} progression being dominant. At 400 nm excitation, most of the excitation goes into higher-lying electronic states or higher members of vibrational progressions.

In the case of $[Ru^{II}(bpy)_3]^{2+}$, the $t = 0$ excitation−emission Stokes shift of 6500 cm^{-1} was attributed to the fact that the

(23) Braterman, P. S.; Song, J. I.; Peacock, R. D. *Inorg. Chem.* **1992**, *31* (4), 555−559.

(24) Schonherr, T.; Degen, J.; Gallhuber, E.; Hensler, G.; Yersin, H. *Chem. Phys. Lett.* **1989**, *158* (6), 519−523.

emission represented one of the maxima of a vibrationally hot progression of the 1607 cm^{-1} mode, due to emission from the $v' = 2$ stationary level of the ^{1}MLCT state. Here the excitation−emission Stokes shift is 8300 cm^{-1}, and the emission spectrum in Figure 2 shows no sign of higher-energy contributions. This implies that if the Stokes shift were dynamical, the upper excited state would be quenched on a time scale of ∼1 fs, which is unphysical. Therefore, and similar to the case of $[Ru^{II}(bpy)_3]^{2+}$, we attribute the singlet emission in $[Fe^{II}(bpy)_3]^{2+}$ to one of the maxima of a progression of vibrationally hot ^{1}MLCT emission. More systematic studies as a function of pump wavelength would be needed to verify this hypothesis. Nevertheless, suffice it to say here that the analogy with $[Ru^{II}(bpy)_3]^{2+}$ leads us to conclude that we are dealing with the ^{1}MLCT emission and that the ^{1}MLCT state undergoes ISC in ≤20 fs, which is supported by the weak ^{3}MLCT emission at ∼660 nm and by the TA measurements. Indeed, these show a short-lived ESA band, which is identical to the reduced bpy ligand (bpy^-) absorption (Figure 4). The bpy^- absorption band peaks in the range between 350 and 370 nm in water, and it can be clearly identified in our data within the first 200 fs after the excitation (Figure 7) as compared to the absorption spectrum of the reduced $[Fe^{II}(bpy)_3]^+$ complex reported in ref 23. Similar to $[Ru^{II}(bpy)_3]^{2+}$,[17,18] this band is assigned to the ^{3}MLCT state, which is formed upon electron transfer (ET) from the metal orbitals to the $\pi-\pi^*$ orbital of the bpy ligand system.[25]

4.2. Population and Decay of the $^5T_2$ (High-Spin) State. From the global fit analysis, we extract a time constant of ∼960 fs (Figures 5 and 7), confirming the previous suggestion that the relaxation time from the initially excited singlet charge-transfer manifold should be ≤1 ps.[14,15,21] However, in these studies, it was concluded that the $^5T_2$ state is directly populated from the ^{1}MLCT state, for which a lifetime of ≤100 fs was estimated (no intermediate absorption or emission were observed in the initial 1 ps following excitation). Here we capture spectrally and kinetically the ^{3}MLCT state, and we kinetically resolve the population of the HS state in ≤1 ps. We believe that the presence of this component in both the ESA absorption ≥550 nm and in the GSB signal is the first clear-cut evidence of the arrival time to the HS state. Furthermore, the analysis of the long-time kinetics confirmed that the long-lived ESA in this range can be explained as the HS absorption that has the same lifetime as the GSB recovery time of 665 ± 35 ps at 523 nm (see Supporting Information Figure S2). This implies that the 1 ns time window is dominated by the GSB recovery signal in the short-wavelength and central part of the spectral window investigated here, while a residual HS state absorption is present in the red-most part of the spectrum (≥560−570 nm in Figure 4).

4.3. Ultrafast Intersystem Crossing. The above results and analysis point to remarkably fast relaxation mechanisms going from the ^{1}MLCT state to the ^{5}T state. Given the excitation energy used here and the zero-point energy of the ^{5}T state,[10] this implies that ∼20 000 cm^{-1} of energy are dissipated in ≤1 ps, i.e., an average of ∼2000 cm^{-1} per 100 fs. Therefore, the relaxation steps occur at close to vibrational times, raising the question of nonadiabatic curve crossing events.[26] The most remarkable of all these steps is the first ultrafast ISC between the ^{1}MLCT and the ^{3}MLCT, which is identical to what we found for $[Ru^{II}(bpy)_3]^{2+}$.[16] This process is on the time scale (≤20 fs) of the highest frequency modes of the molecule, implying that ISC occurs in a strongly non-Born−Oppenheimer regime.

If we consider both complexes (Ru and Fe), we have to reconcile this ultrafast ISC with a number of other, seemingly contradictory, observations:

(a) The highest frequency mode in these systems is the skeleton mode of the bpy ligand at 1607 cm^{-1}, which is dominant in the absorption spectrum (Figure 8 and ref 16), i.e., it couples favorably to the optical excitation. It is also prominent in resonance Raman spectra of the Fe and Ru complexes.[27−29] Also, in the low-temperature absorption spectra, the ^{1}MLCT of the Ru complex shows up as a progression of regularly spaced vibrational levels belonging to this mode,[24] suggesting a quasi-harmonic potential shape. The same holds for the case of the Fe complex, although a detailed analysis of the LT absorption spectrum was not carried out.[5] This means that despite the very strong coupling between singlet and triplet surfaces the vibrational pattern of the singlet state does not seem perturbed, as would be expected in the case of an avoided crossing between two strongly coupled potential energy surfaces.

(b) In the case of $[Ru^{II}(bpy)_3]^{2+}$, from the integrated cross section of its absorption band, we estimate the pure radiative lifetime of the ^{1}MLCT state to be ∼10 ns. The lifetime of the lowest two emitting ^{3}MLCT states are 10 and 230 μs, according to LT emission studies.[30] The singlet and triplet nature of these respective states is clear, but the 10 ns lifetime of the ^{1}MLCT state suggests a slight lengthening compared to a fully allowed electric dipole transition (1−2 ns). This may result from mixing with near-lying longer-lived triplet states and is supported by the appearance of a weak triplet absorption as a red shoulder to the ^{1}MLCT absorption band (Figure S1 of ref 16 and ref 30 for $[Ru^{II}(bpy)_3]^{2+}$ and Figure 8 for $[Fe^{II}(bpy)_3]^{2+}$). In the case of $[Fe^{II}(bpy)_3]^{2+}$, we estimate a comparable radiative lifetime for the ^{1}MLCT state.

(c) The measured ISC rates are identical in the Fe and Ru complexes, although the former has a larger spin−orbit constant.

In order to reconcile these observations, we propose a simple model, depicted in Figure 9, which represents the potential curves associated to the ground state, the ^{1}MLCT and the ^{3}MLCT states as harmonic potentials, as a function of the coordinate that most couples to the optical transition (i.e., the 1607 cm^{-1} skeleton mode of bpy, and other modes). The two excited states have their equilibrium positions, in principle, not much shifted from one another. This is also in line with the fact that both transitions (^{1}MLCT absorption and ^{3}MLCT emission) couple to high-frequency modes of bpy.[16,30,31] Indeed, the Huang−Rhys factors S used to fit the ^{1}MLCT absorption band in the Ru and Fe complexes are ≈0.7[16] and 0.8, respectively, whereas those used to fit the ^{3}MLCT emission in $[Ru^{II}(bpy)_3]^{2+}$ are 0.8−1, depending on the solvent.[31]

(25) Calzaferri, G.; Rytz, R. *J. Phys. Chem.* **1995**, *99* (32), 12141−12150.
(26) Gonzalez, C. R.; Fernandez-Alberti, S.; Echave, J.; Chergui, M. *J. Chem. Phys.* **2002**, *116* (8), 3343−3352.
(27) Clark, R. J. H.; Turtle, P. C.; Strommen, D. P.; Streusand, B.; Kincaid, J.; Nakamoto, K. *Inorg. Chem.* **1977**, *16* (1), 84−89.
(28) Strommen, D. P.; Mallick, P. K.; Danzer, G. D.; Lumpkin, R. S.; Kincaid, J. R. *J. Phys. Chem.* **1990**, *94* (4), 1357−1366.
(29) Webb, M. A.; Knorr, F. J.; McHale, J. L. *J. Raman Spectrosc.* **2001**, *32* (6−7), 481−485.
(30) Yersin, H.; Humbs, W.; Strasser, J. *Coord. Chem. Rev.* **1997**, *159*, 325−358.
(31) Hartmann, P.; Leiner, M. J. P.; Draxler, S.; Lippitsch, M. E. *Chem. Phys.* **1996**, *207* (1), 137−146.

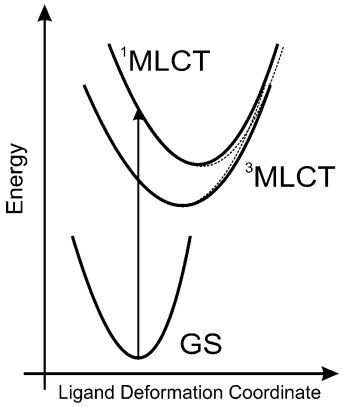

Figure 9. Schematic representation of ground state and the ^{1,3}MLCT potential energy curves. The diabatic ^{1,3}MLCT potentials are drawn with dashed lines, and the adiabatic curves of mixed character, resulting from strong spin−orbit coupling, are represented with solid lines. The most probable (but not unique) ligand deformation coordinate is the one associated to the 1607 cm^{-1} mode.

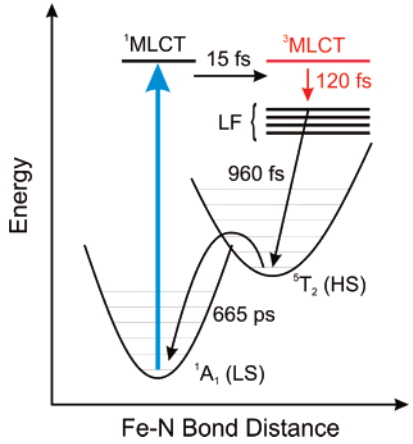

Figure 10. Photophysical cycle of room-temperature aqueous $[Fe^{II}(bpy)_3]^{2+}$. The characteristic lifetimes obtained in the present study are displayed, and the inclusion of ^{3}MLCT in the relaxation cascade is confirmed. The coordinate concerns only to the ground and HS state.

In addition, there should be strong coupling of the two states due to the high spin−orbit constant of the metal atoms. If we consider the coupling constant to be significantly larger than the energy of the high-frequency vibrational modes, this will lead to an avoided crossing, giving rise to adiabatic potential curves (dashed lines) that look quite similar to the diabatic ones, since they cross in a steep region of the potentials. In such a situation, they will maintain a high degree of harmonicity. Because it is quasi-harmonic, the resulting adiabatic curve associated to the ^{1}MLCT will give rise to a progression of quasi-harmonic energy levels. In addition, it will have a mixed character; such that along the deformation coordinate it changes from singlet to triplet (the reverse applies to the triplet state). In our case, in one oscillation of the high-frequency mode, the system crosses over to the adiabatic surface associated to the ^{3}MLCT. That the population does not feed back into the ^{1}MLCT state after one high-frequency oscillation has to do with ultrafast IVR, which occurs by impulsive energy release to lower-frequency modes of the system,[16] so the ISC process is irreversible.

This simple model has the advantage of reconciling the observation of an extremely fast ISC (on the time scale of high-frequency vibrations) with the seemingly harmonic absorption progression. In addition, it supports the observation that the structure at the red edge of the absorption is due to a mixed ^{3}MLCT state, since its intensity is about 10 times weaker that the peak intensity of the ^{1}MLCT absorption band (Figure 8 and Figure S2 of ref 16), whereas we would expect it to ∼1000 weaker, based on the lifetimes mentioned above, if it were a pure triplet state.

Our fit of the ^{1}MLCT absorption bands of the Ru and Fe complexes was made using fwhm values of the individual vibrational bands of the order of 2000 cm^{-1}. This is consistent with the timescales (≤20 fs) we measure for the ISC. However, the LT studies show much narrower line widths of the order of 600−700 cm^{-1},[24,30] implying that the ISC rate is slower in the LT solid. Indeed, one of the implications of the above model is that the ISC rate depends strongly on the relative positions (both in energy and equilibrium distances) of the ^{1}MLCT and ^{3}MLCT surfaces, and these are quite strongly environment dependent.[30,31] Furthermore, it is not excluded that relative equilibrium distances also change from one environment to the other, due to the charge-transfer character of the excited states.[32] Obviously, a direct verification of this hypothesis would be to carry out an excitation energy and solvent dependence study.

The strong S−T mixing implies that the spin and orbital angular momenta are no longer good quantum numbers. During ISC, the total angular momentum of the system ($\Omega = \Lambda + \Sigma$) is conserved, in such a way that the orbital angular momentum is exchanging a quantum with the spin angular momentum. The change of singlet−triplet character is therefore coordinate dependent, and it occurs on the time scale of one vibration. Such dramatic changes of electronic character along a vibrational coordinate are quite common in molecules, and examples are to be found in the change of Rydberg−valence character in the lowest electronic (purely repulsive) state of H_2O[33] and in the change of covalent−ionic character of NaI.[34]

We can now summarize the above results and analysis in the extended relaxation scheme, shown in Figure 10, for the complete photophysical cycle of the solvated $[Fe^{II}(bpy)_3]^{2+}$ complex. After the initial ultrafast ISC, the next step of the relaxation cascade, which we have unraveled here, is the departure from the ^{3}MLCT on a time scale of ∼120 fs. It is not clear to which state (or states) it relaxes, nor which modes are involved in the process, but it is important to note here that all vibrational modes (except the lowest at 283 cm^{-1}) of X−bpy systems (X = Ru, Fe) have relatively high frequencies,[28] i.e., all vibrational periods are <100 fs. In view of this, and although the rates of energy dissipation of ∼2000 cm^{-1}/100 fs are remarkably high, we can conclude that the nonradiative transitions from the ^{3}MLCT to the $^5T_2$ state is a stepwise relaxation process that can be described by the Fermi golden rule, which occurs between stationary levels, contrary to the ^{1}MLCT−^{3}MLCT ISC case above, which is in a strongly non-Born−Oppenheimer regime.

5. Conclusions

We have identified the initial step of the relaxation as an ultrafast ISC from the ^{1}MLCT to the ^{3}MLCT in <20 fs by

(32) Helbing, J.; Chergui, M. *J. Chem. Phys.* **2001**, *115* (13), 6158−6172.
(33) Chergui, M.; Schwentner, N. *Chem. Phys. Lett.* **1994**, *219* (3−4), 237−242.
(34) Cong, P.; Roberts, G.; Herek, J. L.; Mohktari, A.; Zewail, A. H. *J. Phys. Chem.* **1996**, *100* (19), 7832−7848.

femtosecond fluorescence up-conversion and TA measurements. This process occurs in a strongly non-Born−Oppenheimer regime and is mediated by the high-frequency modes of the molecule. Transient absorption studies, coupled with a SVD and GA, have allowed us to identify the relaxation from the ^{3}MLCT in 120 fs, the arrival in the $^5T_2$ state in 960 fs, and the decay of the latter in 665 ps. The whole cascade from the ^{1}MLCT to the $^5T_2$ state corresponds to a dissipation of 2000 cm^{-1}/100 fs, via several ISC and back charge-transfer processes. In spite of being remarkably fast, we believe these steps can be described by the Fermi golden rule where relaxation occurs between stationary levels, contrary to the initial ISC event. These intermediate steps could not be detected in the present experiments, due to lack of spectroscopic observables. We recently detected the $^5T_2$ state by picosecond X-ray absorption spectroscopy and determined its structural parameters (Fe−N bond elongations).[35] With the advent of sources delivering tunable femtosecond X-ray pulses, it will be possible to resolve the intermediate steps within the first picosecond, using X-ray absorption spectroscopy.

Acknowledgment. This work was supported by the Swiss NSF via Contracts 620-066145, 200021-107956, and 200021-105239, the "NCCR:Quantum Photonics". We are grateful to I. Tavernelli (Lausanne) and A. Vlcek (London) for useful discussions.

Supporting Information Available: Experimental methods and setups (fluorescence up-conversion and transient absorption), global analysis procedure, and figure comparing kinetic traces at three different probe wavelengths in the transient absorption. This material is available free of charge via the Internet at http://pubs.acs.org.

JA070454X

(35) Gawelda, W.; Pham, V.-T.; Benfatto, M.; Zaushitsyn, Y.; Kaiser, M.; Grolimund, D.; Johnson, S. L.; Abela, R.; Hauser, A.; Bressler, C.; Chergui, M. *Phys. Rev. Lett.* **2007**, *98*, 057401.